Available online at www.sciencedirect.com
ScienceDirect
Biochimica et Biophysica Acta 1758 (2006) 1450–1460
BIOCHIMICA ET BIOPHYSICA ACTA
BBA
www.elsevier.com/locate/bbamem

Insertion selectivity of antimicrobial peptide protegrin-1 into lipid monolayers: Effect of head group electrostatics and tail group packing

Yuji Ishitsuka [a], Duy S. Pham [b], Alan J. Waring [b,c], Robert I. Lehrer [b], Ka Yee C. Lee [a,*]

[a] *Department of Chemistry, The Institute for Biophysical Dynamics and the James Franck Institute, The University of Chicago, Chicago, IL 60637, USA*
[b] *Department of Medicine, University of California, Los Angeles School of Medicine, Los Angeles, CA 90095, USA*
[c] *Department of Pediatrics, University of California, Los Angeles School of Medicine, Harbor-University of California Los Angeles Medical Center, Torrance, CA 90502, USA*

Received 12 January 2006; received in revised form 31 July 2006; accepted 1 August 2006
Available online 5 August 2006

Abstract

The ability to selectively target the harmful microbial membrane over that of the host cell is one of the most important characteristics of the antimicrobial peptides (AMPs). This selectivity strongly depends on the chemical and structural properties of the lipids that make up the cell membrane. A systematic study of the initial membrane selectivity of protegrin-1 (PG-1), a β-sheet AMP, was performed using Langmuir monolayers. Constant pressure insertion assay was used to quantify the amount of PG-1 insertion and fluorescence microscopy was employed to observe the effect of PG-1 on lipid ordering. Charge and packing properties of the monolayer were altered by using lipids with different head groups, substituting saturated with unsaturated lipid tail group(s) and incorporating spacer molecules. PG-1 inserted most readily into anionic films composed of phosphatidylglycerol (PG) and lipid A, consistent with its high selectivity for microbial membranes. It also discriminated between zwitteranionic phospholipids, inserting more readily into phosphatidylcholine (PC) monolayers than those composed of phosphatidylethanolamine, potentially explaining why PG-1 is hemolytic for PC-rich human erythrocytes and not for the PE-rich erythrocytes of ruminants. Increased packing density of the monolayer by increased surface pressure, increased tail group saturation or incorporation of dihydrocholesterol diminishes the insertion of PG-1. Fluorescence microscopy shows that lipid packing is disordered upon PG-1 insertion. However, the presence of PG-1 can still affect lipid morphology even with no observed PG-1 insertion. These results show the important role that lipid composition of the cell membrane plays in the activity of AMPs.

Keywords: Antimicrobial peptide; Protegrin-1; Langmuir monolayer; Fluorescence microscopy; Peptide–membrane interaction; Model cell membrane; Selectivity; Disordering; Phospholipid; DPPC; DPPE; DPPG; POPC; POPE; POPG; Lipid A; Dihydrocholesterol; Ganglioside

1. Introduction

Antimicrobial peptides (AMPs) are a class of peptides known to protect the host by selectively targeting and disrupting the membrane of harmful microorganisms. They are part of the native immune system of a variety of organisms such as frog (magainin), horseshoe crab (tachyplesin), cow (indolicidin) and human (LL-37 and defensins) and target a wide range of bacteria, fungi, viral infection as well as some tumors[1,2]. AMPs are typically 10–40 amino acids long, containing cationic amino acid residues and adopting an amphiphilic structure when bound to the membrane (α-helical and/or β-sheet). Using their strong membrane affinity, many linear AMPs are known to selectively disrupt the integrity of the target membrane by pore formation via close packed peptides (barrel-stave model) [3–6] or by the assembly of a combination of peptide and lipid molecules (carpet [7–9] and torroidal model [10–12]). This membrane affinity of AMPs does not depend on a specific protein receptor, in contrast to the major histocompatibility complex, as similar antimicrobial activities have been observed even with the counter stereoisomers synthesized using D-amino acids which are not found in nature [6,13–15]. Instead, the overall chemical and structural properties of AMPs are thought to play a more important role. The AMP bactericidal effects can be mimicked by various non-amino-acid-based

* Corresponding author.
E-mail address: kayeelee@uchicago.edu (K.Y.C. Lee).

0005-2736/$ - see front matter © 2006 Elsevier B.V. All rights reserved.
doi:10.1016/j.bbamem.2006.08.001

molecules which possess these chemical and structural properties [16–19].

What then, are the properties of the target membrane that makes it susceptible to the action of AMPs? Prokaryotic cells and eukaryotic cells have distinct membrane lipid composition. The outer leaflet of the mammalian cell membrane is comprised mainly of phosphatidylcholine (PC), sphingomyelin, phosphatidylethanolamine (PE) and cholesterol, which are all charge-neutral at physiological pH [20]. In contrast, bacterial membranes include substantial amounts of negatively charged phospholipids, such as phosphatidylglycerol (PG) and cardiolipin [21]. Furthermore, in Gram-negative bacteria, the outer leaflet of the outer membrane bilayer is composed mostly of lipopolysaccharide (LPS), a polyanionic molecule. Though the potential across the membrane may also contribute, the surface selectivity of cationic AMPs is highly affected by the difference in membrane lipid composition [22,23].

The subtle differences in the lipid composition in various mammalian cell membranes can also result in the differences in their susceptibilities to AMPs. A porcine AMP, protegrin-1 (PG-1), does not lyse the RBCs of sheep, cow and its native host (pig), but can lyse those of human, rabbit and mouse [24]. It should be noted that the concentration required to cause cytotoxicity in mammalian cells is still up to an order of magnitude higher than the minimum inhibitory concentration against bacteria, but the difference in activity towards various mammalian RBCs demonstrates that AMP selectivity is more complex than simple electrostatic interactions between cationic peptide and anionic lipids [24,25].

The basis for the selectivity among mammalian species may be a reflection of the difference in abundance of certain lipids. Phosphatidylethanolamine (PE), for example, accounts for 33.3% of human erythrocyte membrane mass, but composes 47.3% and 67.8% of goat and sheep erythrocytes, respectively [26]. Moreover, phosphatidylcholine (PC) is absent in goat and sheep erythrocyte membranes, but makes up 30.3% of the lipid composition in humans [26,27]. A better understanding of membrane selectivity by these AMPs, such as cecropin [28,29], magainin [30–32] and protegrin [33,34], is important as it can contribute to the development of antibiotic, anti-tumor and anti-infectious agents as well as targeted drug-delivery agents [35]. In this work, we present results on the initial interaction of PG-1 with model cell membranes with different charge and packing characteristics.

PG-1 is an 18 amino acid, amidated peptide (NH_2-RGGRLCYCRRRFCVCVGR-$CONH_2$) originally isolated from porcine leukocytes [36]. Protegrins are part of the porcine immune system, and functionally analogous to defensins in humans [24] and circular (theta) defensins in the rhesus monkey [37]. NMR studies have shown that PG-1 adopts a one-turn β hairpin structure that includes two disulfide bonds [38,39]. This peptide and some of its analogs have a wide range of known targets, including *Escherichia coli* (gram-negative) [36], *Neisseria gonorrhoeae* (gram-negative) [40], *Listeria monocytogenes* (gram-positive) [36], *Candida albicans* (fungi) [41], multidrug-resistant *Mycobacterium tuberculosis* [42] and protects against HIV infection *in vitro* [43].

The apparent membrane disruptive ability of PG-1 was observed with actual bacteria as well as model membrane systems. Electron microscopy study has shown that PG-1 can dramatically disrupt the outer membrane of *Escherichia coli* by the formation of microvilli extending away from the membrane surface [44] and the membrane of *Neisseria gonorrhoeae* by forming cratered structures resembling an active "volcanic terrain" [40]. Among model membrane systems, enhancement of ion permeations in 3:1 1-palmitoyl-2-oleoyl-*sn*-glycero-3-phosphocholine:1-palmitoyl-2-oleoyl-*sn*-glycero-3-[phospho-*rac*-(1-glycerol)] (POPC:POPG) liposomes (1 μg/mL) and planar lipid bilayers containing lipopolysaccharide or lipid A (4 μg/mL) have been shown to increase upon exposure to PG-1 [45].

A number of previous studies has been done to elucidate the mechanism of the membrane disruption ability of PG-1. PG-1 has been found to be stable in a lipid bilayer with a tilted orientation (in multilamellar 1,2-dilauroyl-*sn*-glycero-3-phosphocholine system) [46]. Apart from this favorable peptide–lipid interaction, PG-1 can also oligomerize in the lipid environment [47,48]. When there is a mismatch in thickness between the lipid bilayer and the peptide, the membrane deforms to minimize the hydrophobic mismatch between the peptide and the surrounding lipid tail groups when the peptide-to-lipid ratio reaches a certain threshold value [46,49]. Beyond this threshold concentration, PG-1 and the lipid head group change their relative orientation, suggesting the alteration in the nature of the peptide–lipid interaction and providing a possible signature for pore formation [50,51]. While these studies elucidate the mechanism of membrane disruption, relatively little work has focused on the molecular basis for PG-1 selectivity. In this paper, we present a systematic study on how various membrane properties, such as head group size, head group charge as well as tail group saturation and packing, affect the membrane selectivity of PG-1.

A Langmuir monolayer held at a surface pressure where the lipid packing density is equivalent to that of a lipid bilayer serves as an excellent model for the outer leaflet of the cell membrane [52]. Using a constant pressure insertion assay whereby PG-1 was injected into the aqueous subphase below the monolayer to model the initial interaction of the peptide with the membrane surface, we quantified the amount of PG-1 insertion. The effect of PG-1 insertion on lipid packing was achieved via concurrent monitoring with fluorescence microscopy (FM). In order to address the effect the lipid head group has on PG-1 insertion, we have examined the interaction of PG-1 with lipids that differ only in their head group structures. The effect of tail group packing on PG-1 insertion has been assessed by adjusting the surface pressure, by altering the degree of saturation of the tail groups and by adding spacer molecules that change the fluidity of the film.

2. Materials and methods

2.1. Materials

All phospholipids and ganglioside (G_{M1}) were purchased from Avanti Polar Lipids, Inc. (Alabaster, AL). Diphosphoryl lipid A from *Escherichia coli* F583 (Rd mutant) and dihydrocholesterol (DChol) were purchased from Sigma-Aldrich (St. Louis, MO). All lipids were used without further purification. Appropriate solvents

were used for each lipids to prepare a spreading solution with concentration of 0.1–0.2 mg/ml: chloroform for 1,2-Dipalmitoyl-*sn*-Glycero-3-Phosphocholine (DPPC), 1,2-Dipalmitoyl-*sn*-Glycero-3-Phosphoethanolamine (DPPE), 1-Palmitoyl-2-Oleoyl-*sn*-Glycero-3-Phosphocholine (POPC), 1-Palmitoyl-2-Oleoyl-*sn*-Glycero-3-Phosphoethanolamine (POPE), 1-Palmitoyl-2-Oleoyl-*sn*-Glycero-3-[Phospho-*rac*-(1-glycerol)] (Sodium Salt) (POPG) and DChol; 9:1 chloroform:methanol for 1,2-Dipalmitoyl-*sn*-Glycero-3-[Phospho-*rac*-(1-glycerol)] (Sodium Salt) (DPPG); 74:23:3 chloroform, methanol and water for lipid A. Solvents were obtained from Fisher Scientific (HPLC grade, Pittsburgh, PA). Texas Red, 1,2-dihexadecanoyl*sn*-glycero-3-phosphoethanolamine (TR-DHPE), triethylammonium salt (Invitrogen Co., Carlsbad, CA) was added to make up a solution with 0.5 mol% fluorescent probe. The synthesis of PG-1 has been described elsewhere [39]. 1.0 mg/mL PG-1 was prepared by dissolving in ultra-pure water (resistivity $\geq 18\,M\Omega cm$, Milli-Q, Millipore, Bedford, MA) with 0.01% glacial acetic acid (Fisher reagent grade acetic acid) to prevent aggregation (theoretical pI = 10.66) [53]. Dulbecco's phosphate-buffered saline (D-PBS), without calcium and magnesium (pH = 7.2, Invitrogen Co., Carlsbad, CA), was used for the subphase for all the experiments.

2.2. Langmuir trough and Fluorescence Microscope (FM)

A home-built Langmuir surface balance was used for all surface pressure (Π)–area (A) measurements. Details of this apparatus can be found in a previous publication [54]. In brief, our apparatus consists of a Teflon trough with two symmetric, movable barriers that allow for the control of the area of the monolayer. A Wilhelmy plate made of a filter paper, measures the change in Π accompanied by the change in area. Π is defined as $\gamma_s - \gamma_m$ where γ_m and γ_s are surface tensions of the monolayer and the subphase, respectively. Π (mN/m) and A (Å^2/molecule) were recorded at 1-s interval. The surface tension of the buffer subphase, γ_s, has been approximated to that of the pure water. The temperature control was maintained by a series of thermoelectric units (Omega Engineering Inc, Stamford CT). A water circulator held at 20 °C (Neslab RTE-100; Portsmouth, NH) was coupled to these units to provide a heat sink. A resistively heated indium tin oxide coated glass plate (Delta Technologies, Dallas, TX) was placed over the entire trough to minimize evaporation, dust contamination and condensation on the microscope objective lens. The entire set-up is controlled by a custom software interface designed using Lab View 6.0 (National Instruments, Dallas, TX).

In order to study the surface morphology of our systems concurrently with Π–A isotherm measurements, we used a custom-built fluorescence microscope (FM) with an extra-long working distance 50× objective (Nikon Y-FL, Fryer Co., Huntley, IL) positioned over the Langmuir surface balance. The entire balance was mounted on x, y, and z translational stages for scanning and focusing. The fluorescence emission of TR-DHPE (EX: 530–590 nm; EM: 610–690 nm) premixed in the monolayer was selectively imaged using a filter cube (Nikon HYQ Texas Red, Fryer Co., Huntley, IL). The real time morphological changes were imaged by a charged couple device camera (Cohu Inc., Poway, CA), and recorded on Super-VHS formatted or digital video tapes at video frame rate. FM images were grabbed from video tapes as bitmap images (640 × 480 pixel) using custom image grabbing software. These images were resized and enhanced in brightness and in contrast for clear presentation.

2.3. Surface activity of PG-1

To determine the surface activity of PG-1, surface activity assays were performed in the absence of any lipid at the bare air–buffer interface. Since no lipid monolayer was present at the interface, the area between the two barriers was kept constant during the experiment. The area equivalent to POPG at 30 mN/m (66 Å^2/molecule), with the amount of lipid used for the experiments described in the next section, was selected. Following the surface pressure calibration, peptide solution was injected into the subphase using a syringe with a L-shaped needle. PG-1 concentration ranging between 11.6 nM to 11.6 μM was used. Volume of the injected peptide solution was kept at 2 mL. Immediately after the injection, the surface pressure increased and continued to do so over time. The maximum value was reached within 30 min.

2.4. Constant pressure insertion assay

To quantify the interaction of PG-1 with monolayers, constant pressure insertion studies were carried out. Fig. 1 shows the three steps involved in this assay: monolayer compression, peptide injection and area expansion. Phospholipid and lipid A solutions were spread drop-wise manually at the air–subphase interface using a microsyringe (Hamilton, Reno, NV) to form a monolayer. The total spread volume for each experiment was 50 μL or 100 μL given the concentration of the spreading solutions 0.2 mg/mL and 0.1 mg/mL, respectively. The solvents were allowed to evaporate for 15 min under the atmosphere of constantly streaming argon so that the vapors were purged out of the chamber. For the case of lipid A, the time also allowed the small amount of water needed to dissolve the lipid to be reincorporated into the subphase. Following this step, the monolayer was compressed to a target Π. All the experiments were conducted at pressures close to the bilayer equivalent surface pressure where the lipids are packed at a density similar to that found in a biological membrane [55,56]. The observed insertions therefore are directly relevant to in vivo/physiological conditions. This range of surface pressure is higher than the equilibrium spreading pressure of PG-1 (11.6 μM), thus ensuring that observed area changes are not merely due to the surface activity of the peptide. Upon reaching the target pressure, the pressure was kept constant via a built-in feedback system that adjusted the surface area by moving the barriers. The film was left to equilibrate for 10 min. In all experiments except for the concentration study with POPG (where the peptide concentration ranged from 11.6 nM to 11.6 μM), stock PG-1 solution (1 mg/mL) was injected into the subphase to make up the final PG-1 concentration of 11.6 μM (0.025 mg/mL). This particular concentration was chosen as it is the 50% hemolytic concentration (HC_{50}) for human RBCs. A microsyringe with a L-shaped needle, VDRL needle (Hamilton, Reno, NV), was used to homogeneously spread the mixture below the monolayer. The relative change in area per molecule, $\Delta A/A$, was monitored throughout the experiment. Consequently, $\Delta A/A$ was used to compare the PG-1 insertion into different monolayers. Subphase temperature was maintained at 30 ± 0.5 °C for all experiments. The cover glass temperature was adjusted to be 3 °C above the subphase temperature to prevent condensation.

In order to prevent oxidation, extra precautions have been taken with unsaturated lipid monolayers. The entire trough was sealed in a polyethylene bag (AtmosBag, Sigma-Aldrich, St. Louis, MO) and purged with argon gas (grade 5.0) by repeating three cycles of vacuum suction and argon purging. Everything required for the experiment was placed within the bag before the purging, and all procedures for the experiment were carried out using the two gloves attached to the bag.

3. Results

3.1. Surface activity of PG-1

The surface activity of PG-1 was first investigated at a bare buffer surface. Fig. 2 shows the surface activity of PG-1 depends on peptide concentration (open square). Immediately after injection, Π increased and continued to do so over time. The maximum Π value was reached within 30 min. Each point represents the maximum Π increase after PG-1 injection. With increasing PG-1 concentration, Π increased non-linearly. At 11.6 μM of PG-1, the maximum Π increase was 10.3 mN/m, whereas a mere 0.4 mN/m increase was observed for 116 nM. Further decreasing the concentration to 11.6 nM still resulted in a similar surface pressure increase of 0.4 mN/m, which most likely represented the baseline increase upon injection. The blank injection showed decrease of 0.2 mN/m due to the slight increase of subphase level.

3.2. Concentration dependence of PG-1 insertion into POPG monolayers

Concentration dependence of PG-1 insertion into POPG monolayers was studied at 30 mN/m with PG-1 concentration ranged from 11.6 nM to 11.6 μM. The volume of peptide solution injected (2 mL) was kept constant throughout the study. A new

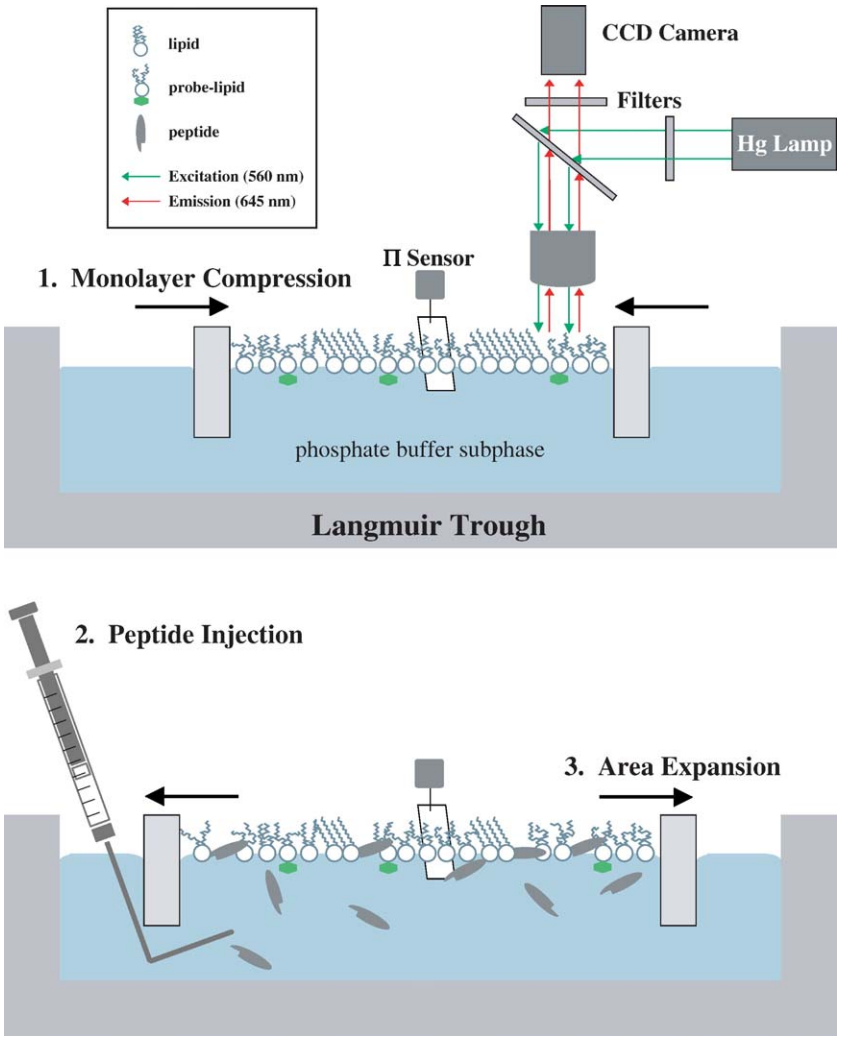

Fig. 1. Constant Pressure Insertion Assay Steps. Shown above are three basic steps of the insertion assay. (1) Monolayer compression: the lipid monolayer at the air–buffer interface is compressed to the target pressure which is comparable to the cell membrane environment. (2) Peptide injection: the peptide solution is slowly and evenly injected below the monolayer using a gas-tight syringe equipped with an L-shaped needle. (3) Area expansion: as a result of peptide insertion, the surface pressure increases. In order to keep the surface pressure constant, the area of the monolayer increases. The Langmuir trough is equipped with two movable barriers. The surface morphology is observed using a fluorescence microscope during the experiment.

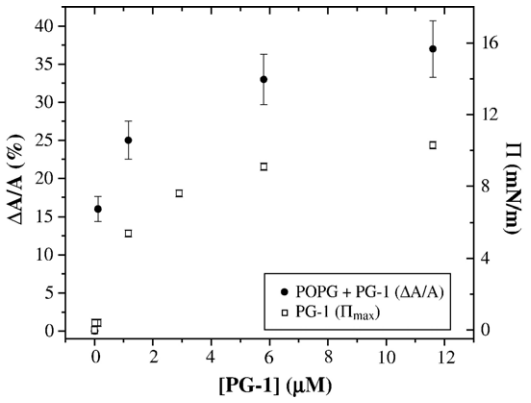

Fig. 2. Surface activity of PG-1 for a bare air–buffer interface (□) and the insertion of PG-1 into POPG monolayers at 30 mN/m (●) are plotted against PG-1 concentration. The data points at 0 and 11.6 nM PG-1 directly overlap one another. Temp = 30 °C; Subphase = D-PBS.

POPG monolayer was spread for each concentration. Each data point represents the maximum $\Delta A/A$ reached between 10 to 100 min after the introduction of the peptide into the subphase. The difference in the time it took to attain steady state was due to the diffusion-limited nature of surface-active molecules reaching the interface [57]. No insertion was observed with blank and 11.6 nM PG-1. A non-linear relationship between PG-1 concentration and PG-1 insertion was observed as shown in Fig. 2 (filled circle).

3.3. PG-1 insertion into monolayers

The capability of PG-1 to insert into DPPE, DPPC and DPPG with fully saturated tails (16:0–16:0, two 16-carbon chain tail groups with zero unsaturation) along with lipid A monolayers was evaluated using the constant pressure insertion assay at various surface pressures in order to understand the head group selectivity of PG-1 along with the effect of lipid tail

group packing on peptide insertion. Fig. 3 shows the result of an insertion assay with a DPPC monolayer held constant at 20 mN/m. Fig. 3A shows a typical *Π–A* isotherm plot. The monolayer was spread at an area beyond the lift off area (95 Å^2/molecule), compressed to the target pressure (20 mN/m) and equilibrated (indicated by arrow 0). PG-1 was injected into the subphase (indicated by arrow 1) and as a result, the surface pressure of the monolayer increased. To relieve the stress, the area also increased over time (indicated by arrow 2) until it reaches a steady state (indicated by arrow 3). Fig. 3B shows the same experiment, but plotting $\Delta A/A$ over time.

Fig. 4 and Table 1 show the amount of PG-1 insertion into various monolayers quantified by the relative area change, $\Delta A/A$, defined as $(A_t - A_i)/A_i \times 100\%$, where A_t is the area per molecule at a given time after PG-1 injection into the subphase and A_i is the area per molecule before PG-1 injection. Each point represents the maximum relative area change, $\Delta A/A$, after the injection of PG-1 into the subphase. The observed kinetics of insertions were non-linear and the maximum value reached within 2 h of peptide injection, depending on the amount of peptide insertion. No insertion was observed with all monolayers upon injection of blank buffer solution.

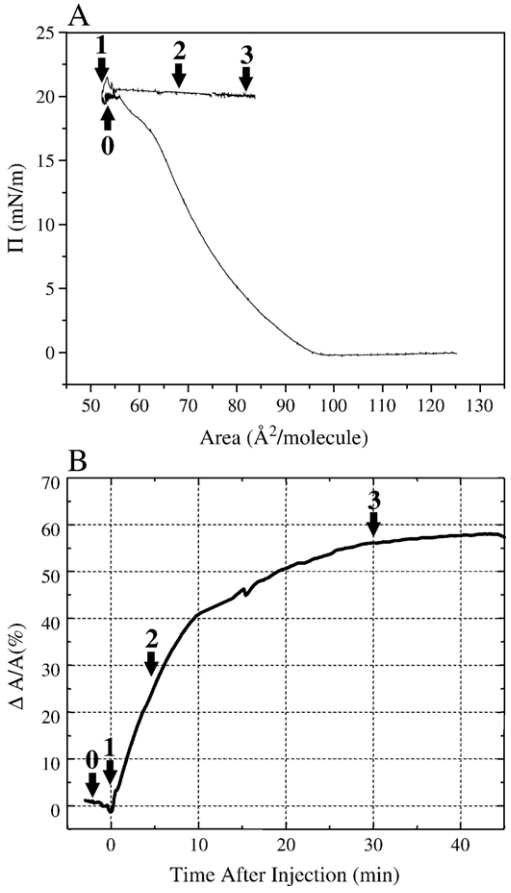

Fig. 3. A Typical Constant Pressure Insertion Isotherm. DPPC/PG-1 at 20 mN/m. A typical isotherm from an insertion assay is shown in two different plots. (A) *Π–A* isotherm: the monolayer was spread at an area beyond the lift off area (95 Å^2/molecule), compressed to the target pressure (20 mN/m) and equilibrated (0). PG-1 was injected into the subphase (1) and as a result, the surface pressure of the monolayer increased. To relieve the stress resulting from the inserted peptide, the area increased over time (2 and 3). (B) $\Delta A/A$ change: the same experiment can be plotted in respect to $\Delta A/A$ over time after injection (1). Temp = 30 °C; subphase = D-PBS.

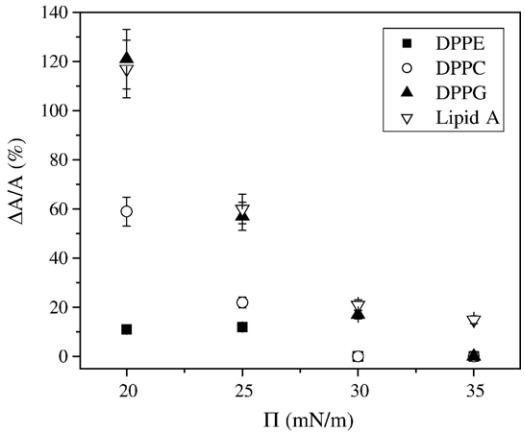

Fig. 4. Maximum relative area change, $\Delta A/A$ (%), attained as a function of the monolayer surface pressure for four different lipids: DPPE (■), DPPC (○), DPPG (▲) and lipid A (▽). Temp = 30 °C; Subphase = D-PBS.

PG-1 insertion into lipid films clearly demonstrated a head group preference. Among the different types of lipid head groups, PG-1 inserted more favorably into anionic DPPG and lipid A monolayers over zwitterionic lipid monolayers. A different amount of PG-1 insertion was observed among zwitterionic lipids. Between zwitterionic DPPC and DPPE monolayers, PG-1 inserted substantially more into DPPC, a lipid with a larger head group. The insertion of PG-1 decreased linearly as a function of increased surface pressure of the monolayer regardless of the type of the monolayer. Higher surface pressure indicates tighter tail group packing. For the case of lipid A, a deviation from the linear decrease was observed at 35 mN/m. At this pressure, PG-1 initially inserted into the lipid A monolayer reaching a maximum area change of 15%. Shortly after the peak, $\Delta A/A$ plummeted to the negative territory over the course of an hour [44].

3.4. Tail group packing studies

While the most abundant lipid tail groups in animal and plant membranes are saturated chains with 14, 16 and 18 carbon atoms [58], unsaturated tail groups are also common components of cell membranes. The effect of substituting one or two of the saturated lipid tail group(s) with a monounsaturated tail group on

Table 1
PG-1 induced relative area change of lipid monolayers

Π (mN/m)	PG-1 Insertion ($\Delta A/A_{max}$)			
	DPPE (+/−)	DPPC (+/−)	DPPG (−)	lipid A (−)
20	11	59	121	117
25	12	22	57	60
30	0	0	17	21
35	0	0	0	15

Maximum relative area change, $\Delta A/A$ (%), of various lipid monolayers held at different constant surface pressures after injection of PG-1. The charge of the head group is indicated in the bracket. [PG-1] = 25 μg/mL (11.6 μM); Temp = 30 °C; Subphase = D-PBS.

PG-1 insertion has been investigated using the constant pressure insertion assay (Table 2). Comparisons were made between DPPE (16:0–16:0) and POPE (16:0–18:1), DPPC (16:0–16:0) and POPC (16:0–18:1), DPPC (16:0–16:0) and DOPC (18:1–18:1), and DPPG (16:0–16:0) and POPG (16:0–18:1). Cartoon representations of unsaturated and saturated lipid molecules are shown at the top and the bottom of the figure, respectively, the ratio of $\Delta A/A$ between unsaturated and saturated lipids are shown in the middle, and surface pressures at which the monolayer was held constant are shown below the insertion ratio.

An overall enhancement of PG-1 insertion was observed in all groups as a result of substituting one saturated tail with an unsaturated tail. The sequential substitution of unsaturated tail group to DPPC resulted in the progressive enhancement of PG-1 insertion in POPC (1.8) and DOPC (2.4). Comparison between DPPG and POPG was carried out at a higher surface pressure because PG-1 inserted into DPPG monolayer even at 30 mN/m, and the effect of unsaturated lipid tail group on PG-1 insertion was found to be further enhanced at 30 mN/m (2.1) compared to that at 25 mN/m (1.3).

The tail group packing density can also be altered by the addition of DChol or G_{M1} to the monolayer. PG-1 insertion assay was tested with 7:3 POPC:DChol monolayer at 30 mN/m and 8:2 DPPC:G_{M1} at 25 mN/m. A different trend was observed between these two systems. The ratio of the relative area change between 7:3 POPC:DChol and POPC at 30 mN/m was 0.2, demonstrating a significant decrease in the PG-1 insertion when DChol was present. Contrary to the effect of DChol, the relative area change between 8:2 DPPC:G_{M1} and DPPC at 25 mN/m was 1.4, signifying an increase in PG-1 insertion with G_{M1} in the film.

Table 2
Enhancement of peptide insertion in the presence of unsaturated tail groups

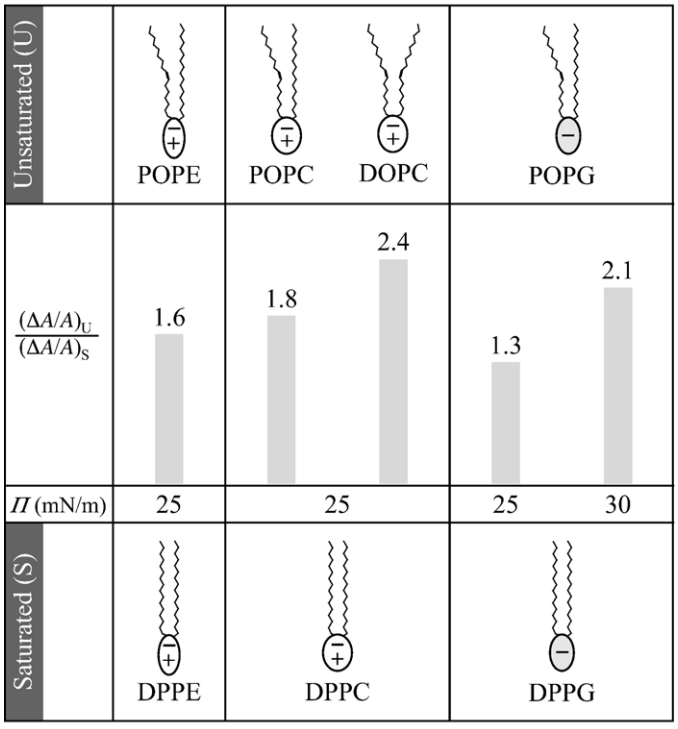

PG-1 insertion into fully saturated (S) lipid monolayers of DPPC, DPPE and DPPG were compared with insertion in lipids with one or two tail groups substituted with unsaturated (U) tail group(s) (POPE, POPC, DOPC, POPG). The effects of tail group substitution are shown by taking the ratio of insertion into the unsaturated lipid monolayer, $(\Delta A/A)_U$, to insertion into the saturated lipid monolayer, $(\Delta A/A)_S$. A number greater than 1 reflects an enhancement of peptide insertion in the unsaturated system. Temp = 30 °C; Subphase = D-PBS.

3.5. Membrane disordering by PG-1

The effect of PG-1 insertion on the morphology of the lipid monolayer was observed using fluorescence microscopy. This technique is applicable when condensed phase is present in the monolayer at the desired surface pressure. Under our experimental conditions, we were able to monitor morphological changes for all saturated phospholipid monolayers (DPPE, DPPC and DPPG). Fig. 5 shows FM images of the monolayer before and after the injection of PG-1 into the subphase. Post injection images were captured after $\Delta A/A$ was reached for each film.

Fluorescent dye tagged lipid, Texas Red-DHPE, favorably partitioned into the less packed liquid phase of the monolayer, leaving the condensed phase dark. In general, the area fraction of the dark condensed phase decreased as PG-1 inserted into the monolayer. This indicates the disordering of lipid packing in the monolayer. Most of the disordering effects took place in the first 10 min, starting at the liquid-condensed phase boundaries. For DPPE, the presence of PG-1 does not result in any significant morphological changes in the film at 25 and 30 mN/m (Fig. 5A–D), indicating little peptide insertion. In contrast, PG-1 alters the morphology and reduces the area fraction of the condensed phase for DPPC (from Fig. 5E–F) and more so for DPPG (Fig. 5I–M), with changes being more drastic at the lower surface pressure. Although no measurable amount of $\Delta A/A$ was recorded, indicating that there is no peptide insertion into the tail portion of the film, an increase in the amount of the brighter phase was observed with DPPC at 30 mN/m. This result indicates that the association of the peptide to the lipid film can give rise to a change in the film's surface in spite of the lack of any detectable peptide insertion by the insertion assay. Fig. 6 shows DPPG monolayer at 25 mN/m 3 min after the injection of PG-1 into the subphase. The progressive blurring of the domains from Fig. 6A–D clearly shows the disordering process at the condensed domain edges. Each image is not at the identical location due to the lateral drift of the monolayer. While extra precaution was taken to homogeneously spread PG-1 solution, different degrees of disordering were observed at different parts of the monolayer, indicating the existence of a certain degree of heterogeneity in PG-1 injection. However, the trends of the surface morphological changes depicted in Figs. 5 and 6 are highly reproducible from experiment to experiment.

4. Discussion

4.1. Concentration-dependent PG-1 activity

There are a number of proposed AMP-induced membrane disordering mechanisms, of which the barrel stave [3–6], the carpet [7–9] and the toroidal model [10–12], are the most

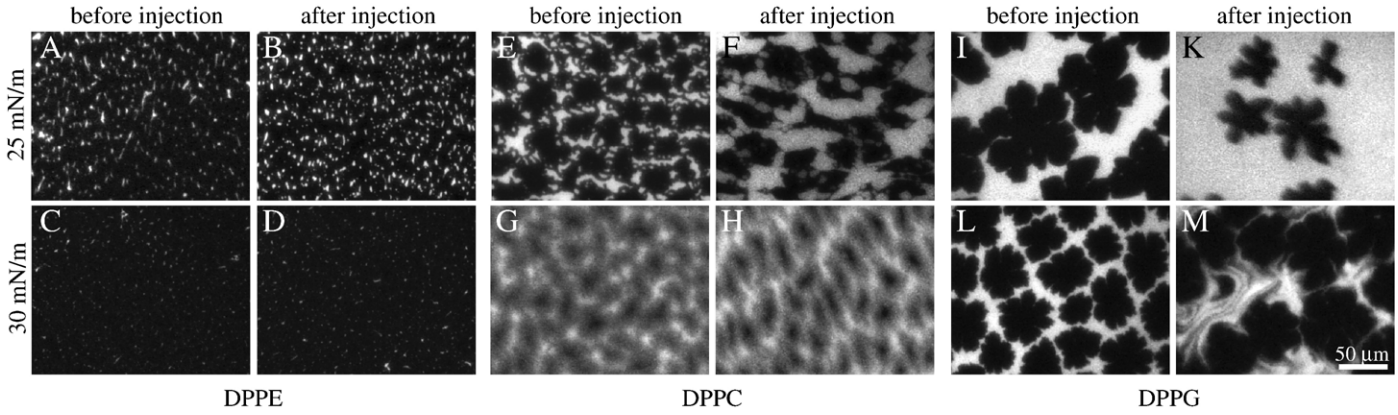

Fig. 5. FM images of DPPE (A–D), DPPC (E–H) and DPPG (I–M) phase morphology before and after the injection of PG-1 beneath the monolayer (between 30–60 min). The surface pressures are 25 and 30 mN/m. Temp = 30 °C; Subphase = D-PBS.

prominent. No single model seems to explain the mechanisms of over hundreds of peptide sequences that are classified as AMPs. However, one common requirement to all AMPs' mechanism in membrane disordering is that the peptide initially adsorbs onto the cell membrane from the extracellular media. It is likely that once the AMPs accumulate on the surface beyond a certain concentration threshold, they may cooperatively insert themselves into the membrane to induce membrane disordering. Recently, we have also directly observed the disruptive effects of PG-1 in supported lipid bilayers using atomic force microscopy [59].

As shown in Fig. 2, the activity of PG-1 with POPG monolayer is highly concentration-dependent. The insertion of PG-1 into a POPG monolayer at 30 mN/m was observed at all concentrations beyond the lowest concentration (11.6 nM). While the surface activity of PG-1 and the insertion of PG-1 into a POPG monolayer show a correlation to each other, a much sharper increase in PG-1 insertion was observed at lower PG-1 concentration range. In particular, the surface pressure increase with 116 nM PG-1 was merely 0.4 mN/m with a bare air–buffer interface, yet a significant amount of insertion (16%) was observed in the presence of POPG monolayer for the same peptide concentration. The concentration dependence of AMPs has been reported to be sigmoidal with alamethicin and δ-lysin [23,60], exhibiting a sharp transition from a surface associated state to an inserted state at certain threshold concentrations. Our results indicate a similar sharp transition for PG-1 in its ability to insert into the POPG film. While no insertion was observed at 11.6 nM, PG-1 inserts readily into the lipid film at a subphase concentration of 116 nM. The sharp concentration dependence of PG-1 activity is an important characteristic for the peptide to possess in order to function as an effective antimicrobial agent. In multilamellar lipid system where the peptide and the lipid are premixed, PG-1 exhibits a sharp transition in its orientation with respect to the lipid [50], and is capable of inducing a sudden change in the head group conformation beyond a certain lipid to peptide ratio [46].

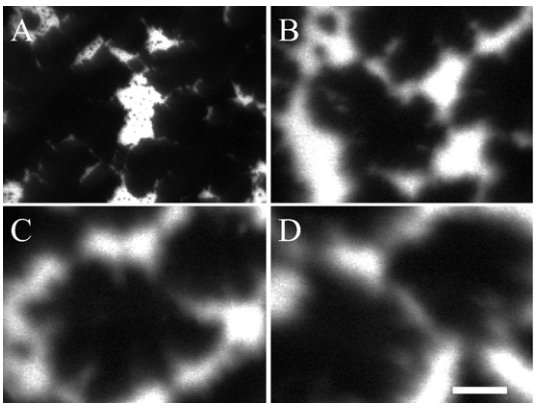

Fig. 6. PG-1 induced packing disordering initiates at the liquid-condensed phase boundary. FM images of DPPG monolayer were captured 3 min after the injection of PG-1 into the subphase. The progressive blurring of the domains from A–D clearly shows the disordering process at the condensed domain edges. Scale bar = 50 μm; Π = 25 mN/m; Temp = 30 °C; Subphase = D-PBS.

In order to evaluate the differences in PG-1 ability to insert into various monolayers, it is important to ensure that the constant pressure assays are conducted at pressures higher than the pressure attainable by the peptide in the absence of any lipid film. This allows us to distinguish between the surface activity of peptide from lipid/peptide interaction. Indeed, our surface activity study of the peptide at the bare air–buffer interface shows that the maximum surface pressure attained with 11.6 μM of PG-1 in the subphase was 10.3 mN/m, a pressure much lower than the ones used for our insertion assays.

4.2. Head group selectivity

The head group of the membrane lipid is the first portion of the membrane encountered by PG-1. Consequently, the chemical properties of the head group, specifically the electrostatic property and the size of the head group, play an important role in the membrane selectivity of PG-1.

The highest degree of PG-1 insertion was observed in lipids with anionic head groups, DPPG and lipid A. The origin of this preferential interaction comes from the electrostatic attraction between the cationic PG-1 (+7) and these anionic lipids. Lipid A is the lipid anchor of lipopolysaccharide that is found at the outer membrane of Gram-negative bacteria, and lipids with the PG head group are predominant in the plasma membrane of

both Gram-negative and Gram-positive bacteria. On the other hand, only zwitterionic lipids are found in the outer leaflet of the mammalian RBC membrane. Due to favorable electrostatic interactions, the presence of anionic lipids increases the local concentration of PG-1 at the monolayer surface. Consequently, a higher degree of insertion is observed with anionic compared to zwitterionic lipid films. An additional contribution of the anionic head group to PG-1 insertion comes from the charge–charge repulsion between neighboring head groups. The repulsion between anionic head groups increases the effective head group size making them more accessible for the insertion of PG-1's.

The differences obtained in the PG-1 insertion among zwitterionic lipids (PC vs. PE) show that electrostatics of the head group alone cannot explain the observed selectivity. Comparing lipids with saturated tails and their unsaturated counterparts, we find that PG-1 inserts more favorably into monolayers with PC head groups over PE head groups. One explanation for this preference for PC is the head-tail mismatch of the lipid. The cross sectional diameter of the PC head group is larger than that of the two saturated tail groups, whereas that of PE is smaller. With DPPC, the large head group prevents lipid tails to pack as tightly as those in DPPE held at identical surface pressure and subphase conditions [61]. As demonstrated from X-ray reflectivity results, the tail groups of DPPC tilt even at relatively high surface pressures, resulting in a rectangular unit cell [52]. On the other hand, DPPE molecules are able to pack tightly with the tails arranged in a hexagonal unit cell at comparable pressure [62]. Tightly packed tail groups of DPPE thus prevent PG-1 to effectively insert into the monolayer. While the membranes of mammalian RBCs are constituted by similar lipid species, the ratio of these species differ among pigs, sheep and human. Sheep RBC contains a higher amount of PE lipids and a lower amount of PC lipids compared to human RBC. Both factors contribute towards protecting the cell from peptide insertion. This difference in the lipid composition of the cell membrane may explain the difference in PG-1 susceptibility among mammalian species.

4.3. PG-1 insertion into various tail group packing

The insertion results obtained using monolayers with various tail group packing clearly point to the effects of tail group packing density on peptide insertion. Similar to the head group size effect discussed above, an increase in tail group packing tends to decrease PG-1 insertion. This effect is apparent when the packing density of the lipid tail groups is increased by increasing the surface pressure of the monolayer (Fig. 4). The decrease in PG-1 insertion appears to be linear for all lipids examined except for the lipid A monolayer at high surface pressure. At 35 mN/m, a quick initial increase in the area of the lipid A monolayer indicates the insertion of PG-1. However, instead of maintaining the increased area, the film decreases in its area, indicating a possible loss of material into the subphase. The area decrease may also take place as a result of rearrangement of lipid molecules in the monolayer held at a constant surface pressure, but the rate of area decrease post PG-1 insertion is significantly faster than the area decrease observed for molecular rearrangement. The insertion of PG-1 into the lipid A monolayer possibly increases the solubility of the lipid A molecules, leading to the destabilization of the lipid film by the process of micellization. This is plausible since the solubility of lipid A in aqueous phase is higher than other phospholipids indicated by the requirement of a more hydrophilic solvent for its dissolution (see Materials). This solubilized structure is perhaps similar to the vesicle/micelle phase recently observed through NMR with POPC:POPG system, but not with pure POPC system, after addition of PG-1 [63]. A possible micellization process has also been observed with using a linear AMPs pardaxin and magainin [64,65].

There are a number of ways in which the cell membrane regulates the packing density of its membrane components, and unsaturation of the tail group is one of them. Comparison of the degree of PG-1 insertion between DPPC, POPC and DOPC clearly shows an increase in PG-1 insertion as more unsaturated tail groups are present in the film. The double bond gives rise to a kink in the unsaturated lipid tail group, preventing the close packing of the tails. Unlike DPPC, Π–A plots for both POPC and DOPC monolayers do not exhibit a liquid to condensed phase transition under our experimental conditions (data not shown). The looser packing created by the unsaturated tail group thus allows PG-1 to insert into the monolayer more easily.

While PG-1 insertion is enhanced by lipid tail unsaturation, the opposite effect is observed when the cholesterol is present in the lipid film. Cholesterol is an integral component in the mammalian cell membrane. Structurally it is a rather flat molecule. Its sterol rings can fit nicely in the lipid tail region and its hydroxyl group helps to anchor it at the lipid head–tail interface. In effect, cholesterol can be thought of as an intercalator in the lipid film, functioning as a spacer to compensate the head–tail size mismatch and increase the packing density of the tail region. It is therefore not surprising that PG-1 inserts less into a POPC/DChol compared with a POPC monolayer. From the binding energy study of cationic peptide LamB-W (a cationic analog of the LamB signal peptide), addition of 40% cholesterol to egg-PC vesicle system resulted in a decrease in the binding energy by 1.5 kcal/mol [66].

Addition of 20% G_{M1} to DPPC, on the other hand, has led to an increase in PG-1 insertion. The observed increase is likely due to the competition between two opposing effects brought about by the addition of G_{M1}: lipid packing and surface charge. G_{M1} is a glycolipid commonly present in the mammalian cell membrane as a signaling molecule, and it has a large penta-saccharide attached to two acyl tail groups. The large sugar groups may be thought of as hindering lipid packing due to steric hindrance, but the addition of 20% G_{M1} to a DPPC monolayer in fact acts to allow the lipids to pack more tightly and lowers the phase transition surface pressure (data not shown). This means that the 8:2 DPPC:G_{M1} monolayer has a higher content of the condensed phase than the pure DPPC monolayer. This condensing effect of G_{M1} has been observed in the Π–A plot of the monolayer as well as the earlier appearance of the condensed phase in FM images. The lack of a phosphate group

in the head group region most likely allows G_{M1} to act as a spacer between the large head group of DPPC molecules and enhance the lipid packing. As discussed earlier, this increase in packing density would decrease PG-1 insertion. On the other hand, the sialic acid on one of the sugar groups in G_{M1} adds a negative charge to the surface. As we discussed earlier, this acts to increase the local concentration of PG-1 near the monolayer, and hence the insertion of PG-1. Despite of the increased packing effect of G_{M1}, the enhanced observed insertion shows that local accumulation of peptides along the surface brought about by the G_{M1} plays a stronger role in PG-1 activity.

4.4. PG-1 lipid packing disordering

The fact that the membrane insertion of PG-1 disorders the lipid tail group packing is clearly demonstrated by the decrease in the area fraction of the dark condensed phase for DPPE, DPPC and DPPG at 25 mN/m (Fig. 5B, F, K) and DPPG at 30 mN/m (Fig. 5M) after the injection of PG-1. No morphological change was seen upon PG-1 injection in DPPE monolayer at 30 mN/m due to the closely packed tail groups (Fig. 5D). Although no detectable $\Delta A/A$ was measured with DPPC at 30 mN/m, a small morphological change was observed (Fig. 5H). This demonstrates that PG-1 is surface-associated, but cannot penetrate into the monolayer at this surface pressure.

The disordering process is initiated at the liquid-condensed phase boundary. As seen in the blurring of the condensed phase domains in Fig. 6, the peptide first inserts into the liquid phase and then destabilizes the condensed phase, using the boundary as a weak point for insertion. One of the driving forces for PG-1 insertion is the hydrophobic matching between the peptide and the lipid tail group. X-ray reflectivity data have previously shown that when PG-1 inserts, it spans through both the head group and tail group regions of the lipid monolayer [44]. The condensed domains observed in FM images originate from the nucleation of closely packed tail groups of lipid molecules. Deeply penetrated PG-1 acts to melt these domains by associating with the surrounding tail groups. Strong tail group–peptide interaction has been suggested by the membrane thinning effect observed with multilamellar lipid systems [49]. The findings of this work suggest that when the thickness of the lipid bilayer (~4 nm) is thicker than the length of the peptide (3 nm when fully extended), the acyl chains deforms to match the hydrophobic regions of the inserted peptide. The length scale of such thickness deformation ranges from several angstroms [49] to nanometer scale [67]. In our insertion assay, the area of the monolayer expands in order to compensate for the increased surface pressure due to PG-1 insertion. The area increase is due to the presence of the peptide in the lipid film, which leads to an effective increase in the area-per-molecule occupied by the lipids. Furthermore, peptide insertion disorders the lipid film, resulting in a similar deformation of the tail group.

5. Conclusion

Our results delineate several important membrane properties that affect the initial membrane selectivity of PG-1. The ability of PG-1 to initially associate with and insert into a lipid film exhibits a sharp dependence on peptide concentration. Given the same overall peptide concentration, the local concentration of PG-1 at the membrane surface is greatly enhanced by the presence of anionic lipid molecules that are prevalent in the bacterial membrane. Highest degree of PG-1 insertion has been observed with anionic lipid monolayers, while zwitterionic lipids only show a moderate amount of insertion at low surface pressure. The packing density of the lipid plays an important role in PG-1 insertion. Systematically altering the way the lipid molecules pack by changing the surface pressure, substituting saturated with unsaturated tail groups, and adding DChol and G_{M1} to the film, shows that the packing density is inversely proportional to the amount of PG-1 insertion. Our PG-1 insertion study using the Langmuir monolayer thus provides a clear demonstration of the effect of individual chemical and physical properties on the membrane selectivity of PG-1.

Acknowledgements

K.Y.C.L. is grateful for the support of the Packard Foundation (99-1465), the University of Chicago MRSEC Program of the NSF (DMR0213745) and the Alfred P. Sloan Foundation (BR-4028). The experimental apparatus was made possible by National Science Foundation Chemistry Research Instrumentation and Facility/Junior Faculty Grant (CHE-9816513).

References

[1] M. Zasloff, Antimicrobial peptides of multicellular organisms, Nature 415 (2002) 389–395.
[2] N. Papo, Y. Shai, A molecular mechanism for lipopolysaccharide protection of Gram-negative bacteria from antimicrobial peptides, J. Biol. Chem. 280 (2005) 10378–10387.
[3] B. Christensen, J. Fink, R.B. Merrifield, D. Mauzerall, Channel-forming properties of cecropins and related model compounds incorporated into planar lipid membranes, Proc. Natl. Acad. Sci. U. S. A. 85 (1988) 5072–5076.
[4] G. Ehrenstein, H. Lecar, Electrically gated ionic channels in lipid bilayers, Q. Rev. Biophys. 10 (1977) 1–34.
[5] K. He, S.J. Ludtke, D.L. Worcester, H.W. Huang, Neutron scattering in the plane of membranes: structure of alamethicin pores, Biophys. J. 70 (1996) 2659–2666.
[6] P. Juvvadi, S. Vunnam, R.B. Merrifield, Synthetic melittin, its enantio, retro, and retroenantio isomers, and selected chimeric analogs: their antibacterial, hemolytic, and lipid bilayer action, J. Am. Chem. Soc. 118 (1996) 8989–8997.
[7] Y. Pouny, D. Rapaport, A. Mor, P. Nicolas, Y. Shai, Interaction of antimicrobial dermaseptin and its fluorescently labeled analogues with phospholipid membranes, Biochemistry 31 (1992) 12416–12423.
[8] Y. Shai, Mechanism of the binding, insertion and destabilization of phospholipid bilayer membranes by alpha-helical antimicrobial and cell non-selective membrane-lytic peptides, Biochim. Biophys. Acta 1462 (1999) 55–70.
[9] M. Wu, E. Maier, R. Benz, R.E. Hancock, Mechanism of interaction of different classes of cationic antimicrobial peptides with planar bilayers and with the cytoplasmic membrane of *Escherichia coli*, Biochemistry 38 (1999) 7235–7242.
[10] S.J. Ludtke, K. He, W.T. Heller, T.A. Harroun, L. Yang, H.W. Huang, Membrane pores induced by magainin, Biochemistry 35 (1996) 13723–13728.
[11] K. Matsuzaki, O. Murase, N. Fujii, K. Miyajima, An antimicrobial peptide, magainin 2, induced rapid flip-flop of phospholipids coupled

with pore formation and peptide translocation, Biochemistry 35 (1996) 11361–11368.
[12] A. Mor, P. Nicolas, The NH2-terminal alpha-helical domain 1–18 of dermaseptin is responsible for antimicrobial activity, J. Biol. Chem. 269 (1994) 1934–1939.
[13] M. Dathe, M. Schumann, T. Wieprecht, A. Winkler, M. Beyermann, E. Krause, K. Matsuzaki, O. Murase, M. Bienert, Peptide helicity and membrane surface charge modulate the balance of electrostatic and hydrophobic interactions with lipid bilayers and biological membranes, Biochemistry 35 (1996) 12612–12622.
[14] Z. Oren, Y. Shai, Selective lysis of bacteria but not mammalian cells by diastereomers of melittin: structure–function study, Biochemistry 36 (1997) 1826–1835.
[15] D. Wade, A. Boman, B. Wahlin, C.M. Drain, D. Andreu, H.G. Boman, R.B. Merrifield, All-D amino acid-containing channel-forming antibiotic peptides, Proc. Natl. Acad. Sci. U. S. A. 87 (1990) 4761–4765.
[16] L. Arnt, K. Nusslein, G.N. Tew, Nonhemolytic abiogenic polymers as antimicrobial peptide mimics, J. Polym. Sci., A, Polym. Chem. 42 (2004) 3860–3864.
[17] D.H. Liu, W.F. DeGrado, De novo design, synthesis, and characterization of antimicrobial beta-peptides, J. Am. Chem. Soc. 123 (2001) 7553–7559.
[18] J.A. Patch, A.E. Barron, Helical peptoid mimics of magainin-2 amide, J. Am. Chem. Soc. 125 (2003) 12092–12093.
[19] E.A. Porter, B. Weisblum, S.H. Gellman, Mimicry of host–defense peptides by unnatural oligomers: antimicrobial beta-peptides, J. Am. Chem. Soc. 124 (2002) 7324–7330.
[20] S.L. Keller, W.H. Pitcher III, W.H. Huestis, H.M. McConnell, Red blood cell lipids form immiscible liquids, Phys. Rev. Lett. 81 (1998) 5019–5022.
[21] C. Ratledge, S.G. Wilkinson, Microbial Lipids, vol. 1, Academic Press, London, 1988.
[22] K. Matsuzaki, K. Sugishita, N. Fujii, K. Miyajima, Molecular basis for membrane selectivity of an antimicrobial peptide, magainin 2, Biochemistry 34 (1995) 3423–3429.
[23] F.Y. Chen, M.T. Lee, H.W. Huang, Sigmoidal concentration dependence of antimicrobial peptide activities: a case study on alamethicin, Biophys. J. 82 (2002) 908–914.
[24] L. Bellm, R.I. Lehrer, T. Ganz, Protegrins: new antibiotics of mammalian origin, Expert Opin. Investig. Drugs 9 (2000) 1731–1742.
[25] N. Ostberg, Y. Kaznessis, Protegrin structure–activity relationships: using homology models of synthetic sequences to determine structural characteristics important for activity, Peptides 26 (2005) 197–206.
[26] M.H. Nouri-Sorkhabi, L.C. Wright, D.R. Sullivan, P.W. Kuchel, Quantitative 31P nuclear magnetic resonance analysis of the phospholipids of erythrocyte membranes using detergent, Lipids 31 (1996) 765–770.
[27] M.H. Nouri-Sorkhabi, N.S. Agar, D.R. Sullivan, C. Gallagher, P.W. Kuchel, Phospholipid composition of erythrocyte membranes and plasma of mammalian blood including Australian marsupials; quantitative 31P NMR analysis using detergent, Comp. Biochem. Physiol., Part B: Biochem. Mol. Biol. 113 (1996) 221–227.
[28] H.M. Chen, W. Wang, D. Smith, S.C. Chan, Effects of the anti-bacterial peptide cecropin B and its analogs, cecropins B-1 and B-2, on liposomes, bacteria, and cancer cells, Biochim. Biophys. Acta 1336 (1997) 171–179.
[29] H. Steiner, D. Hultmark, A. Engstrom, H. Bennich, H.G. Boman, Sequence and specificity of two antibacterial proteins involved in insect immunity, Nature 292 (1981) 246–248.
[30] M.A. Baker, W.L. Maloy, M. Zasloff, L.S. Jacob, Anticancer efficacy of magainin2 and analog peptides, Cancer Res. 53 (1993) 3052–3057.
[31] R.A. Cruciani, J.L. Barker, M. Zasloff, H.C. Chen, O. Colamonici, Antibiotic magainins exert cytolytic activity against transformed cell lines through channel formation, Proc. Natl. Acad. Sci. U. S. A. 88 (1991) 3792–3796.
[32] M. Zasloff, Magainins, a class of antimicrobial peptides from *Xenopus* skin: isolation, characterization of two active forms, and partial cDNA sequence of a precursor, Proc. Natl. Acad. Sci. U. S. A. 84 (1987) 5449–5453.
[33] D.A. Mosca, M.A. Hurst, W. So, B.S. Viajar, C.A. Fujii, T.J. Falla, IB-367, a protegrin peptide with in vitro and in vivo activities against the microflora associated with oral mucositis, Antimicrob. Agents Chemother. 44 (2000) 1803–1808.
[34] G. Drin, J. Temsamani, Translocation of protegrin I through phospholipid membranes: role of peptide folding, Biochim. Biophys. Acta 1559 (2002) 160–170.
[35] N. Papo, Y. Shai, Host defense peptides as new weapons in cancer treatment, Cell. Mol. Life Sci. 62 (2005) 784–790.
[36] V.N. Kokryakov, S.S. Harwig, E.A. Panyutich, A.A. Shevchenko, G.M. Aleshina, O.V. Shamova, H.A. Korneva, R.I. Lehrer, Protegrins: leukocyte antimicrobial peptides that combine features of corticostatic defensins and tachyplesins, FEBS Lett. 327 (1993) 231–236.
[37] Y.Q. Tang, J. Yuan, C.J. Miller, M.E. Selsted, Isolation, characterization, cDNA cloning, and antimicrobial properties of two distinct subfamilies of alpha-defensins from rhesus macaque leukocytes, Infect. Immun. 67 (1999) 6139–6144.
[38] A. Aumelas, M. Mangoni, C. Roumestand, L. Chiche, E. Despaux, G. Grassy, B. Calas, A. Chavanieu, Synthesis and solution structure of the antimicrobial peptide protegrin-1, Eur. J. Biochem. 237 (1996) 575–583.
[39] R.L. Fahrner, T. Dieckmann, S.S. Harwig, R.I. Lehrer, D. Eisenberg, J. Feigon, Solution structure of protegrin-1, a broad-spectrum antimicrobial peptide from porcine leukocytes, Chem. Biol. 3 (1996) 543–550.
[40] X.D. Qu, S.S. Harwig, A.M. Oren, W.M. Shafer, R.I. Lehrer, Susceptibility of Neisseria gonorrhoeae to protegrins, Infect. Immun. 64 (1996) 1240–1245.
[41] Y. Cho, J.S. Turner, N.N. Dinh, R.I. Lehrer, Activity of protegrins against yeast-phase *Candida albicans*, Infect. Immun. 66 (1998) 2486–2493.
[42] L. Fattorini, R. Gennaro, M. Zanetti, D. Tan, L. Brunori, F. Giannoni, M. Pardini, G. Orefici, In vitro activity of protegrin-1 and beta-defensin-1, alone and in combination with isoniazid, against Mycobacterium tuberculosis, Peptides 25 (2004) 1075–1077.
[43] H. Tamamura, T. Murakami, S. Horiuchi, K. Sugihara, A. Otaka, W. Takada, T. Ibuka, M. Waki, N. Yamamoto, N. Fujii, Synthesis of protegrin-related peptides and their antibacterial and anti-human immunodeficiency virus activity, Chem. Pharm. Bull. (Tokyo) 43 (1995) 853–858.
[44] D. Gidalevitz, Y.J. Ishitsuka, A.S. Muresan, O. Konovalov, A.J. Waring, R.I. Lehrer, K.Y.C. Lee, Interaction of antimicrobial peptide protegrin with biomembranes, Proc. Natl. Acad. Sci. U. S. A. 100 (2003) 6302–6307.
[45] Y. Sokolov, T. Mirzabekov, D.W. Martin, R.I. Lehrer, B.L. Kagan, Membrane channel formation by antimicrobial protegrins, Biochim. Biophys. Acta 1420 (1999) 23–29.
[46] S. Yamaguchi, T. Hong, A. Waring, R.I. Lehrer, M. Hong, Solid-state NMR investigations of peptide–lipid interaction and orientation of a beta-sheet antimicrobial peptide, protegrin, Biochemistry 41 (2002) 9852–9862.
[47] J.J. Buffy, A.J. Waring, M. Hong, Determination of peptide oligomerization in lipid bilayers using F-19 spin diffusion NMR, J. Am. Chem. Soc. 127 (2005) 4477–4483.
[48] C. Roumestand, V. Louis, A. Aumelas, G. Grassy, B. Calas, A. Chavanieu, Oligomerization of protegrin-1 in the presence of DPC micelles. A proton high-resolution NMR study, FEBS Lett. 421 (1998) 263–267.
[49] W.T. Heller, A.J. Waring, R.I. Lehrer, T.A. Harroun, T.M. Weiss, L. Yang, H.W. Huang, Membrane thinning effect of the beta-sheet antimicrobial protegrin, Biochemistry 39 (2000) 139–145.
[50] W.T. Heller, A.J. Waring, R.I. Lehrer, H.W. Huang, Multiple states of beta-sheet peptide protegrin in lipid bilayers, Biochemistry 37 (1998) 17331–17338.
[51] R. Mani, A.J. Waring, R.I. Lehrer, M. Hong, Membrane-disruptive abilities of beta-hairpin antimicrobial peptides correlate with conformation and activity: a 31P and 1H NMR study, Biochim. Biophys. Acta 1716 (2005) 11–18.
[52] C. Ege, K.Y. Lee, Insertion of Alzheimer's A beta 40 peptide into lipid monolayers, Biophys. J. 87 (2004) 1732–1740.
[53] E. Gasteiger, C. Hoogland, A. Gattiker, D. S., W. M.R., R.D. Appel, A. Bairoch, in: J.M.W. Walker (Ed.), The Proteomics Protocols Handbook, Humana Press, 2005, pp. 571–607.

[54] A. Gopal, K.Y.C. Lee, Morphology and collapse transitions in binary phospholipid monolayers, J. Phys. Chem., B 105 (2001) 10348–10354.
[55] A. Seelig, Local anesthetics and pressure: a comparison of dibucaine binding to lipid monolayers and bilayers, Biochim. Biophys. Acta 899 (1987) 196–204.
[56] T. Soderlund, J.M. Alakoskela, A.L. Pakkanen, P.K. Kinnunen, Comparison of the effects of surface tension and osmotic pressure on the interfacial hydration of a fluid phospholipid bilayer, Biophys. J. 85 (2003) 2333–2341.
[57] H. Diamant, G. Ariel, D. Andelman, Kinetics of surfactant adsorption: the free energy approach, Colloids Surf., A Physicochem. Eng. Asp. 183 (2001) 259–276.
[58] W.W. Christie, Lipid Analysis; Isolation, Separation, Identification, and Structural Analysis of Lipids, 3rd ed.The Oily Press, Bridgwater, England, 2003.
[59] K.L.H. Lam, Y. Ishitsuka, Y. Chen, K. Chien, A.J. Waring, R.I. Lehler, K.Y.C. Lee, Mechanism of Membrane Disruption by Antimicrobial Peptide PG-1, Journal of Physical Chemistry B (in press).
[60] M. Bhakoo, T.H. Birkbeck, J.H. Freer, Interaction of *Staphylococcus aureus* delta-lysin with phospholipid monolayers, Biochemistry 21 (1982) 6879–6883.
[61] P. Somerharju, J.A. Virtanen, K.H. Cheng, Lateral organisation of membrane lipids. The superlattice view, Biochim. Biophys. Acta 1440 (1999) 32–48.
[62] J. Majewski, T.L. Kuhl, K. Kjaer, G.S. Smith, Packing of ganglioside–phospholipid monolayers: an X-ray diffraction and reflectivity study, Biophys. J. 81 (2001) 2707–2715.
[63] R. Mani, J.J. Buffy, A.J. Waring, R.I. Lehrer, M. Hong, Solid-state NMR investigation of the selective disruption of lipid membranes by protegrin-1, Biochemistry 43 (2004) 13839–13848.
[64] B. Bechinger, Detergent-like properties of magainin antibiotic peptides: a P-31 solid-state NMR spectroscopy study, Biochim. Biophys. Acta, Biomembr. 1712 (2005) 101–108.
[65] K.J. Hallock, D.K. Lee, J. Omnaas, H.I. Mosberg, A. Ramamoorthy, Membrane composition determines pardaxin's mechanism of lipid bilayer disruption, Biophys. J. 83 (2002) 1004–1013.
[66] T.J. McIntosh, A. Vidal, S.A. Simon, The energetics of binding of a signal peptide to lipid bilayers: the role of bilayer properties, Biochem. Soc. Trans. 29 (2001) 594–598.
[67] A. Janshoff, D.T. Bong, C. Steinem, J.E. Johnson, M.R. Ghadiri, An animal virus-derived peptide switches membrane morphology: possible relevance to nodaviral transfection processes, Biochemistry 38 (1999) 5328–5336.